Transverse Nuclear Spin Relaxation Studies of Viscoelastic Properties of Membrane Vesicles. II. Experimental Results

Gerhard Althoff,[†] Oliver Stauch,[‡] Marija Vilfan,[§] Diego Frezzato,[||] Giorgio J. Moro,[||] Philipp Hauser,[†] Rolf Schubert,[‡] and Gerd Kothe*[,†]

Department of Physical Chemistry, University of Freiburg, Albertstrasse 21, D-79104 Freiburg, Germany, Department of Pharmaceutical Technology, University of Freiburg, Hermann-Herder-Strasse 9, D-79104 Freiburg, Germany, J. Stefan Institute, Jamova 39, 1000 Ljubljana, Slovenia, and Department of Physical Chemistry, University of Padova, Via Loredan 2, I-35131 Padova, Italy

Received: July 23, 2001; In Final Form: March 4, 2002

Transverse nuclear spin relaxation measurements employing Carr−Purcell (CP) pulse sequences have been used to determine the viscoelastic properties of quasi-spherical membrane vesicles with controlled radii R_0. The observed relaxation rates, $R_2^{CP}(\omega)$, exhibit a linear dependence on the inverse pulse frequency over a wide frequency range in the kHz regime and then level off to a constant "plateau" value independent of ω. Within the linear dispersion regime, the same relaxation rates are detected for unilamellar and oligolamellar vesicles, indicating that the interbilayer coupling is weak and has no effect on the measured relaxation curves. Analysis of the experimental dispersion profiles is performed using a slow-motional model in which two different relaxation processes are considered (i.e., vesicle shape fluctuations and molecular translational diffusion). It is shown that for vesicle radii $R_0 \geq 200$ nm lateral diffusion across the vesicle shell is too slow to contribute significantly to transverse spin relaxation in the kHz range. Rather, vesicle shape fluctuations constitute the dominant transverse relaxation process. Model calculations reveal that $R_2^{CP}(\omega)$, induced by vesicle fluctuations, depends linearly on ω^{-1} over a wide frequency range in the kHz regime. Notably, within this linear dispersion regime, the bending elastic modulus κ is the only relevant parameter because the magnitude of $R_2^{CP}(\omega)$ does not depend on R_0, the effective lateral tension σ, and the viscosity of the surrounding fluid η. On the other hand, R_0, σ, η, and κ determine the frequency at which $R_2^{CP}(\omega)$ levels off to a constant plateau value. Thus, analysis of the linear dispersion regime is a direct way to determine the bending rigidity κ. For the studied DMPC and DMPC/cholesterol vesicles, the κ values vary from $(1.5 \pm 0.1) \times 10^{-20}$ J to $(8.3 \pm 0.1) \times 10^{-20}$ J. From the plateau in the experimental dispersion profiles, values for the effective lateral tension of $\sigma = 3 \pm 1$ and 4 ± 1 have been extracted. It appears that transverse NMR relaxation involving CP sequences represents a powerful tool for the study of the viscoelastic properties of membrane vesicles.

1. Introduction

Biological cells are enclosed by an outer membrane that controls the transfer of ions, molecules, and molecular aggregates between the extracellular space and the cytosol. The core of any biomembrane is the lipid bilayer to which the glycocalix and the cytoskeleton are attached on the extra- and intracellular sides, respectively. The bilayer may be regarded as a matrix set up by amphiphilic lipid molecules into which other membrane constituents such as proteins are embedded.

Because of their amphiphilic nature, phospholipids spontaneously form closed-shell bilayers (i.e., membrane vesicles). Depending on the method of preparation, these vesicles may have membranes consisting of a single bilayer or several adjacent bilayers. A schematic representation of such a vesicle is shown in Figure 1. Vesicles represent simple model systems for compartment formation in biological cells. Moreover, vesicles are well-suited to study the exceptional viscoelastic properties of membranes and are unequaled by any other soft condensed matter material.[1]

The viscoelastic nature of biomembranes gives rise to thermally excited vesicle fluctuations, which can be observed directly by video microscopy of giant unilamellar vesicles. Fourier analysis of the fluctuating contours provides values for the bending elastic modulus, κ, of the membranes.[2−8] Nuclear magnetic resonance (NMR) relaxation studies of oligolamellar lipid dispersions are well-suited to supplement the video microscopy techniques by extending the accessible frequency range of fluctuations.[9−12]

The first NMR detection of vesicle fluctuations was achieved by measuring longitudinal nuclear spin relaxation rates, $R_1(\omega_0)$, at low Larmor frequencies, ω_0,[9] using a field-cycling technique.[13] This method, however, is experimentally demanding and suffers from local field effects at low external fields. These problems are circumvented by measuring transverse spin relaxation rates, $R_2^{CP}(\omega)$,[14] in Carr−Purcell−Meiboom−Gill (CP) sequences.[15] Here, ω denotes the pulse frequency that is defined as the inverse pulse spacing in the CP pulse train.

A theoretical basis for the NMR studies was given by Marqusee et al.[16] who calculated the nuclear spin relaxation rate due to out-of-plane fluctuations (i.e., undulations of a planar

* To whom correspondence should be addressed. E-mail: kothe@pc1.chemie.uni-freiburg.de. Fax: 0049-761-2036222.
[†] Department of Physical Chemistry, University of Freiburg.
[‡] Department of Pharmaceutical Technology, University of Freiburg.
[§] J. Stefan Institute.
[||] University of Padova.

10.1021/jp012829l CCC: $22.00
Published on Web 05/04/2002

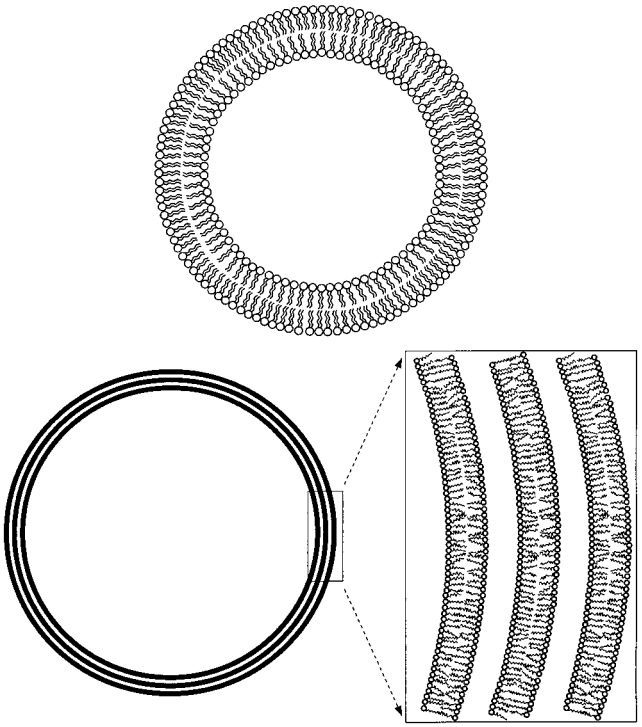

Figure 1. Schematic representation of a unilamellar (top) and an oligolamellar vesicle (bottom). The ^{31}P probe nuclei used in this study are located in the headgroups of the lipid molecules.

membrane). They found that longitudinal spin relaxation induced by planar membrane undulations depends linearly on the Larmor frequency, $R_1(\omega_0) \propto \omega_0^{-1}$, in the same manner as it does in thermotropic liquid crystals with a layered structure.[17] Indeed, this linear dispersion behavior was observed experimentally in the kHz regime by measuring $R_2^{CP}(\omega)$ as a function of ω for multilamellar stacks of planar membranes[14] and for oligolamellar dispersions of various lipids.[10−12] Later, however, doubts were raised about the ability of NMR to determine the bending elastic modulus in these systems, as the intermembrane coupling might limit the free-membrane undulations to the upper MHz regime where they are hardly observable anymore.[18] It was indicated that the range of the linear dispersion regime depends on the transverse orientational correlation length of the membrane, on the number of bilayers in the stack, and on the dispersion relation for the damping times of the fluctuation modes.[19]

To avoid the uncertainty induced by so many unknown parameters in the analysis of experimental NMR data, a spin relaxation study of unilamellar quasi-spherical vesicles has recently been proposed.[20] Using Redfield theory, it was shown that the fluctuation modes of these vesicles give rise to spin relaxation rates, with a linear dispersion regime extending down to the kHz range.[20] This result provides a direct way to determine the bending elastic modulus and other viscoelastic parameters of membrane vesicles. However, because the damping times of the fluctuation modes extend to the millisecond range, the use of a fast-motion theory for the analysis of transverse nuclear spin relaxation is no longer justified, and one should resort to a slow-motional approach. Such a formal treatment of the dynamic problem has been presented in the preceding paper for the specific case of ^{31}P nuclei in the headgroups of lipid molecules.[21]

In this paper, we report experimental studies of the transverse ^{31}P nuclear spin relaxation rates of dimyristoylphosphatidylcholine (DMPC) vesicles in excess of aqueous buffer. First, results are presented for unilamellar DMPC vesicles, where the problem of interbilayer interactions does not exist (see Figure 1). The observed relaxation rates, $R_2^{CP}(\omega)$, depend linearly on ω^{-1} over a wide frequency range in the kHz regime. Then, we present $R_2^{CP}(\omega)$ data for oligolamellar DMPC vesicles measured at the same temperature. Notably, the observed values for $R_2^{CP}(\omega)$ are identical to those obtained for the unilamellar DMPC vesicles in the linear dispersion regime. Finally, we show the $R_2^{CP}(\omega)$ dispersion profiles for oligolamellar DMPC/cholesterol vesicles measured at three different temperatures. Again, a linear dependence of $R_2^{CP}(\omega)$ on ω^{-1} is observed in the kHz regime. However, the absolute values of $R_2^{CP}(\omega)$ now differ considerably from those obtained in the previous case.

The experimental results can be interpreted in terms of a transverse NMR relaxation model that was developed in the preceding paper.[21] It was shown that for vesicle radii $R_0 \geq 200$ nm thermally excited vesicle fluctuations constitute the dominant transverse relaxation process.[21] The model predicts a linear dependence of $R_2^{CP}(\omega)$ on ω^{-1} over a wide frequency range in the kHz regime. Within this linear dispersion regime, the magnitude of $R_2^{CP}(\omega)$ should be independent of the size of the vesicle R_0, the effective lateral tension σ, and the viscosity of the surrounding fluid η, leaving the bending elastic modulus κ as the only relevant parameter.[20,21] On the other hand, R_0 σ, η, and κ are predicted to determine the frequency at which $R_2^{CP}(\omega)$ levels off to a constant plateau value independent of ω.[20,21] Thus, analysis of the experimental $R_2^{CP}(\omega)$ dispersion profiles on the basis of this model can provide values for a variety of viscoelastic parameters of lipid vesicles. The results are discussed in relation to previous studies of the viscoelastic properties of membranes, which are of major importance in the understanding of the biological membrane function.

2. Experiments and Methods

Sample Preparation. Unilamellar vesicles were obtained by a detergent removal technique. A 5:1 mol/mol mixture of the detergent *n*-octyltetraoxyethylene and DMPC was dissolved in 99.9% ethanol. The solvent was removed by rotary evaporation at 313 K followed by thoroughly drying under high vacuum (2×10^{-2} mbar, 2 h). The dry lipid film was dispersed in a 330 mmol/l HEPES (2-[4-(2-hydroxyethyl)-1-piperazino]ethanesulfonic acid) buffer at pH = 7.4 (293 K). The detergent was removed by 72 h of dialysis at 313 K in a MiniLipoprep Dialyzer (Dianorm GmbH, Munich) equipped with a Diachema cellulose acetate membrane (molecular mass cutoff: 10 kDa). The dialysis chamber rotated at 4 cps. The buffer was replaced three times the first day and once during the following two days. Size fractionation of the vesicles was achieved by several centrifugation steps (2500 *g*, 45 min). After concentration of the sample by ultracentrifugation (35 000 *g*, 30 min), the lipid dispersion was transferred into an NMR tube (5.0−7.5 mm o.d.) and sealed with a Teflon plug.

Oligolamellar vesicles were prepared by an extrusion technique. Pure DMPC or a DMPC/30% cholesterol mixture (mol/mol) was dissolved in 99.9% ethanol. The solvent was removed, and the dry lipid film was dispersed in HEPES buffer as described above for the unilamellar vesicles. The dispersion was repeatedly (10−15 times) extruded through a polycarbonate membrane with pore sizes of 0.4−0.8 μm in an Avestin Liposofast extruder at 313 K. For the NMR measurements, the dispersion was treated as described above.

Sample Characterization. The number of bilayers in the membrane of a vesicle (i.e., the lamellarity) was determined by transmission electron microscopy (TEM), using a Zeiss Omega EM912 microscope (Zeiss, Oberkochen). Negative

staining with 2% ammonium molybdate yielded vesicle preparations in which the single bilayers of the membrane were resolved. In detergent-dialyzed DMPC samples, about 70% of the vesicles were unilamellar. The remaining vesicles exhibited mainly two bilayers, resulting in an average lamellarity of about 1.4. Extruded DMPC vesicles showed 1−10 bilayers, yielding an average lamellarity of about 3.1. For extruded DMPC/cholesterol vesicles, a lamellarity of 3.5 was found.

The vesicle radii R_0 were determined by dynamic light scattering (photon correlation spectroscopy) using a Zeta Master S (Malvern, Herrenberg) spectrometer. This method is best suited for small vesicles. For the medium-sized vesicles (240 nm $\leq R_0 \leq$ 520 nm) studied in this work, the given radii should be regarded as estimates rather than exact values. The phospholipid concentration was determined according to Bartlett. [22] It ranged from 40−100 mmol/L depending on sample preparation and vesicle size.

NMR Measurements. The NMR measurements were performed on a Bruker Avance DSX 300 spectrometer operating at ^{31}P and ^{1}H frequencies of 121.5 and 300.13 MHz, respectively. A static solid-state probe with proton decoupling was used in all experiments. The probe was equipped with a doubly tuned solenoid coil for 7.5- or 5.0-mm o.d. samples. The 90° pulse width was set to 3.5 μs for ^{31}P and to 3.0 μs for ^{1}H. All measurements were carried out with proton decoupling in the rotating frame (spin-lock decoupling)[23] at a 6.5-kHz power level.

Transverse ^{31}P spin relaxation rates, $R_2^{CP}(\omega)$, were determined using a CP echo pulse train[15] (i.e., $(\pi/2)_x - [\tau - (\pi)_y - \tau]_n$) with an eight-step phase-cycling scheme. Depending on the relaxation rate, the pulse spacing, and the sample, 8−200 pulses were applied in a single pulse train. The whole CP experiment was recorded starting immediately before the $(\pi/2)_x$ excitation pulse. The digitization interval (dwell time) was set from 5 to 10 μs. Depending on the signal-to-noise ratio, up to 8192 single transients were accumulated.

The intensity of an individual echo maximum was determined by fitting the experimental echo curve by either orthogonal polynomials or cubic splines whose parameters were chosen to fit the data within experimental error as judged by the χ^2 criterion.[24] The error was estimated as the root-mean-square noise of the final part of the echo train curve.

Generally, only the even-numbered echoes were used for the evaluation of the relaxation rates, $R_2^{CP}(\omega)$. On these echoes, unavoidable pulse width errors are canceled to first order.[15] Because vesicle samples were used, the orientational dependence of $R_2^{CP}(\omega)$ was evaluated by a deconvolution procedure.[11] Details of this procedure are given in the next section.

The sample temperature was set with a stream of thermostated nitrogen gas. For this purpose, a Bruker BVT 3000 temperature control unit was used. The temperature stability was better than ±0.5 K.

Computations. Fortran 77 programs were written for the evaluation of the anisotropic relaxation rates $R_2^{CP}(\omega)$ and the viscoelastic parameters κ and σ. The fit programs are based on the nonlinear least squares subroutine LSQMAR of Brandt[25] that uses the Levenberg−Marquardt algorithm[24,25] for searching parameter space and employs singular value decomposition to achieve numerically stable calculations. The performance of the programs was improved by supplying the necessary derivatives analytically.

3. Experimental Results

The principal aim of the experiments described here is the evaluation of viscoelastic properties of membrane vesicles using transverse ^{31}P spin relaxation in CP multipulse sequences. It was pointed out in the preceding paper that the nuclear spin relaxation rates, $R_2^{CP}(\omega)$, depend on the orientation, θ_B, of the average local membrane normal (average director) with respect to the magnetic field,[21] provided that lateral translational diffusion is too slow to average the relaxation rates of the whole vesicle. The observed ^{31}P NMR spectra (see Figure 2) clearly show that this averaging does not occur. Vesicles can therefore be treated as isotropic powders where all orientations θ_B are represented, and a deconvolution procedure is required to extract the relaxation rate for a particular orientation.

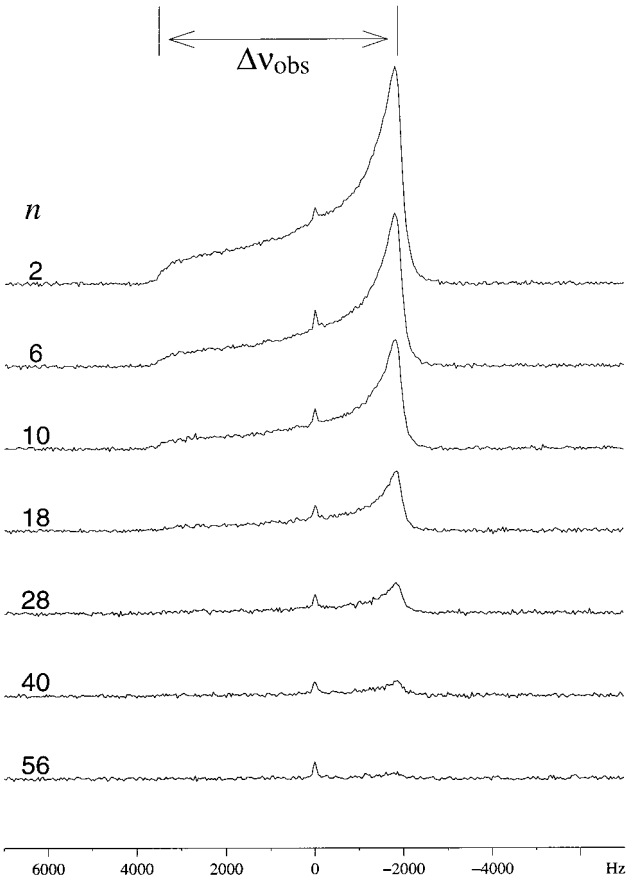

Figure 2. Partially relaxed ^{31}P NMR spectra obtained for oligolamellar DMPC vesicles at 313 K. The seven line shapes are obtained by Fourier transformation of the nth echoes of a Carr−Purcell sequence with a pulse spacing of $\tau = 125$ μs.

Anisotropic Relaxation Rates. In principle, it is possible to determine the anisotropy of $R_2^{CP}(\omega)$ by Fourier transforming the final echoes of CP trains for different numbers of echoes, n, at each pulse frequency. Figure 2 shows partially relaxed ^{31}P NMR spectra of the oligolamellar DMPC sample using a CP pulse train. The line shapes refer to $T = 313$ K and a pulse spacing of $\tau = 125$ μs. The number of echoes after which the Fourier transformation has been performed is indicated on the corresponding spectrum. Note that the shoulder at 3.5 kHz corresponds to the $\theta_B = 0°$ orientation, whereas the singularity that appears at about −1.7 kHz originates from those microdomains in which the average director is oriented 90° to the magnetic field. From the separation of the singularities in the ^{31}P powder spectrum, the observed splitting, $\Delta\nu_{obs}$, can be determined.

Inspection of the line shapes in Figure 2 reveals that the 0 and 90° orientations relax most slowly. A more quantitative analysis of the $R_2^{CP}(\omega)$ anisotropy can be performed by fitting

series of line shapes, such as those in Figure 2, using the general form

$$R_2^{CP}(\omega) = \frac{1}{4}(3\cos^2\theta_B - 1)^2 A_0 + 3\sin^2\theta_B\cos^2\theta_B A_1 + \frac{3}{4}\sin^4\theta_B A_2 \quad (1)$$

where the A's are free adjustable parameters. This general form for the anisotropy of $R_2^{CP}(\omega)$ is exactly correct within the motional narrowing limit. However, eq 1 may be usefully applied in any regime, provided that for each individual orientation θ_B the spins relax monoexponentially. This behavior can also be expected in the case of slow vesicle fluctuations except for the canonical orientations $\theta_B = 0$ and 90°.[21]

The outlined deconvolution procedure, however, is time- and labor-intensive, and an alternative method has been employed to extract the desired information. For the homogeneous samples studied in this work, it is possible to exploit eq 1 so that the measured amplitude $M(2n\tau)$ of the nth echo in a CP experiment is

$$M(2n\tau) = M_0 \int_0^1 \exp\left\{-\left[\frac{1}{4}(3\cos^2\theta_B - 1)^2 A_0 + 3\sin^2\theta_B\cos^2\theta_B A_1 + \frac{3}{4}\sin^4\theta_B A_2\right]2n\tau\right\} \mathrm{d}\cos\theta_B \quad (2)$$

and the decay curve for a given pulse spacing τ may be fitted by independently varying the four parameters M_0, A_0, A_1, and A_2. In the actual case, the number of fitting parameters is effectively reduced to two. The initial amplitude M_0 can be estimated from the amplitude of the first echoes measured at short pulse spacings where the initial decay is slow. Furthermore, eq 1 predicts a marked anisotropy of $R_2^{CP}(\omega)$ only if all three terms do not contribute significantly. As a consequence, there are usually only two of the parameters out of A_0, A_1, and A_2 to fit.

Typical echo decay curves and corresponding fits based on eq 2 are shown in Figure 3. They refer to the oligolamellar DMPC sample at $T = 313$ K for three different pulse spacings τ. Only the even-numbered echoes are depicted, and for each data set, a representative error bar is given. It can be seen that eq 2 reasonably fits the experimental decay curves over nearly three orders of magnitude in echo amplitude. The obtained values for A_0, A_1, and A_2 were used to calculate the largest relaxation rate, which we assign to the $\theta_B = 45°$ orientation. This assignment is justified by inspection of the partially relaxed ^{31}P powder spectra (see Figure 2), which indicate the fastest decay at the 45° orientation.

Dispersion Profiles. Figure 4 shows transverse ^{31}P nuclear spin relaxation rates $R_2^{CP}(\omega)$ as functions of pulse frequency ω for pure DMPC vesicles. The ^{31}P relaxation rates were measured at $T = 313$ K using the standard CP pulse sequence [15] with spin-lock proton decoupling.[23] Results are shown for unilamellar (open squares) and oligolamellar vesicles (filled diamonds) with well-defined vesicle radii of $R_0 = 425$ and 240 nm, respectively. In each case, the dispersion profiles refer to the $\theta_B = 45°$ orientation that was extracted from the CP echo decays using eq 2.

Two remarkable features are obtained from the results in Figure 4. First, both relaxation curves exhibit a linear dependence of the transverse relaxation rate on the pulse frequency ($R_2^{CP}(\omega) \propto \omega^{-1}$) over more than one frequency decade in the kHz regime. Moreover, at low frequencies, a plateau appears in the $R_2^{CP}(\omega)$ dispersion plots. This plateau is clearly visible for the oligolamellar DMPC sample (filled diamonds) that is characterized by the smaller vesicle radius of $R_0 = 240$ nm (see Table 1).

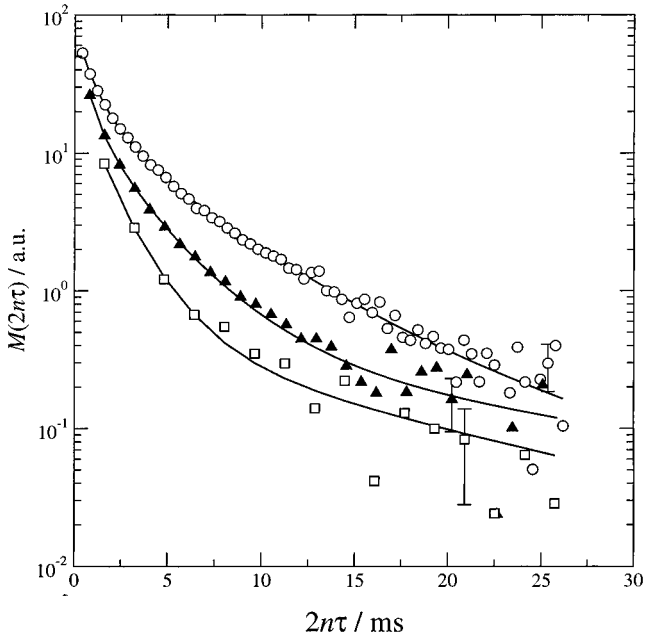

Figure 3. Decay of the transverse ^{31}P magnetization in a Carr−Purcell sequence for oligolamellar DMPC vesicles at 313 K. The decay curves refer to three different pulse spacings τ: (○), $\tau = 100$ μs; (▲), $\tau = 200$ μs; (□), $\tau = 400$ μs. Only the even-numbered echoes are shown. For each data set, a representative error bar is given. The solid lines represent best-fit simulations using the general expression for the anisotropy of the transverse nuclear spin relaxation rate $R_2^{CP}(\omega)$.

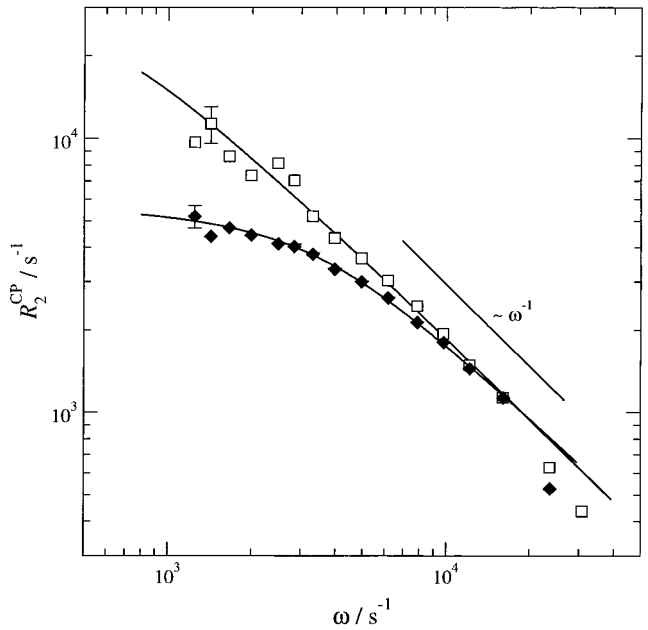

Figure 4. Dependence of the transverse ^{31}P nuclear spin relaxation rate $R_2^{CP}(\omega)$ on the pulse frequency ω in a Carr−Purcell sequence for unilamellar (□) and oligolamellar (◆) DMPC vesicles at 313 K. The dispersion profiles refer to two different vesicle radii: $R_0 = 425$ nm (□) and $R_0 = 240$ nm (◆). For each data set, a representative error bar is given. The solid lines represent best-fit simulations using a transverse NMR relaxation model for shape fluctuations of quasi-spherical vesicles. The underlying parameters are listed in Table 1.

The second notable aspect of the results in Figure 4 is that the relaxation rates $R_2^{CP}(\omega)$ are, within the linear dispersion regime, the same for the unilamellar and the oligolamellar vesicles. Thus, we find that the interbilayer coupling is weak

TABLE 1: Parameters Used in the Analysis of Pulse Frequency-Dependent Transverse ^{31}P Nuclear Spin Relaxation Rates from Carr−Purcell Sequences[a]

	sample				
parameter	DMPC/HEPES[b] buffer unilamellar[c]	DMPC/HEPES[b] buffer oligolamellar[d]	DMPC/30% choles./HEPES[b] buffer oligolamellar[e]	DMPC/30% choles./HEPES[b] buffer oligolamellar[e]	DMPC/30% choles./HEPES[b] buffer oligolamellar[e]
temperature, T/K	313	313	313	303	293
observed splitting[f], $\Delta\nu_{obs}$/kHz	5.34	5.34	5.48	5.73	5.90
viscosity[g], $\eta/10^{-4}$ Pa s	6.5	6.5	6.5	8.0	10.0
vesicle radius[h], R_0/nm	425	240	520	520	520
intermolecular distance[i], a/nm	1	1	1	1	1
director orientation[j], θ_B/deg	45	45	45	45	45
bending modulus[k], $\kappa/10^{-20}$ J	1.7 ± 0.1	1.5 ± 0.1	2.8 ± 0.1	4.7 ± 0.1	8.3 ± 0.1
lateral tension[k], σ	3 ± 1	4 ± 1	≈ 0	≈ 0	≈ 0
excess area[l], $\Delta A/A_{sphere}$	0.13	0.13	0.08	0.05	0.03
order parameter[m], S_{ODF}	0.60	0.60	0.74	0.85	0.92

[a] Parameters characterize the shape fluctuations of quasi-spherical vesicles and refer to different samples. [b] HEPES: 2-[4-(2-hydroxyethyl)-1-piperazino]ethanesulfonic acid. [c] Average lamellarity 1.4. [d] Average lamellarity 3.1. [e] Average lamellarity 3.5. [f] Extracted from experimental ^{31}P NMR spectra (see Figure 2). [g] Viscosity of water. [h] Determined by dynamic light scattering. [i] See eq 5. [j] θ_B denotes the angle between the average diretor and the external magnetic field. [k] Cited errors are linear confidence limits (confidence level 0.95). [l] Relative excess area is given by $\Delta A/A_{sphere} = \Delta/4\pi$ (see eq 9). [m] Order parameter of the fluctuating membrane normal (see eq 12).

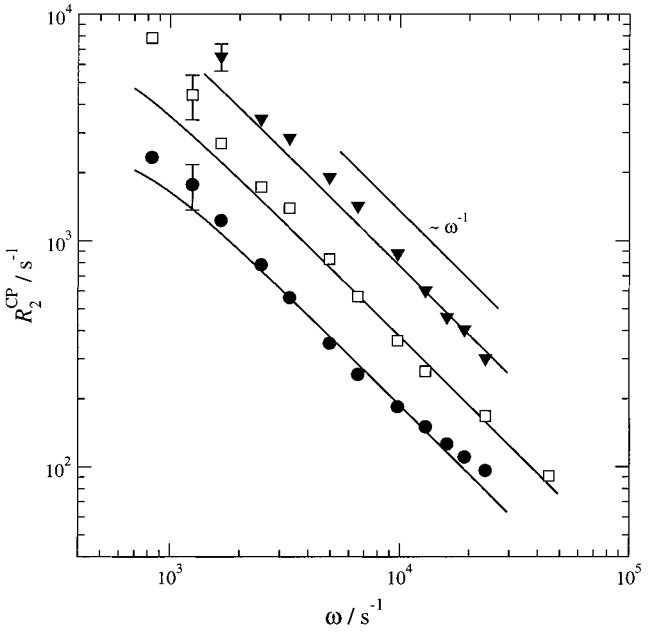

Figure 5. Dependence of the transverse ^{31}P nuclear spin relaxation rate $R_2^{CP}(\omega)$ on the pulse frequency ω in a Carr−Purcell sequence for oligolamellar DMPC/30% cholesterol vesicles at 313 K. The dispersion profiles refer to $T = 313$ K (▼), 303 K (□), and 293 K (●) and a vesicle radius of $R_0 = 520$ nm. For each data set, a representative error bar is given. The solid lines represent best-fit simulations using a transverse NMR relaxation model for shape fluctuations of quasi-spherical vesicles. The underlying parameters are listed in Table 1.

for fluctuations in the NMR frequency range and has no effect on the measured dispersion profiles. This result indicates that the model developed for the analysis of unilamellar vesicles[21] might also be used for oligolamellar vesicles.

Figure 5 shows transverse ^{31}P nuclear spin relaxation rates for oligolamellar DMPC/30 mol % cholesterol vesicles at three different temperatures between 313 and 293 K. The dispersion profiles refer to the $\theta_B = 45°$ orientation and a vesicle radius of $R_0 = 520$ nm. Again, a linear dispersion law of $R_2^{CP}(\omega) \propto \omega^{-1}$ is observed in the kHz regime. However, the absolute values of $R_2^{CP}(\omega)$ now are significantly smaller than those obtained for the pure DMPC vesicles (see Figure 4). Notably, there is a pronounced decrease of $R_2^{CP}(\omega)$ with decreasing temperature. A similar temperature effect was observed also for the pure DMPC vesicles (results not shown).

4. Data Analysis

NMR studies of slow motions in membrane vesicles have focused principally on two types of processes, namely, lateral diffusion across a curved surface and vesicle shape fluctuations. Both of these mechanisms have been considered in the preceding paper using a comprehensive transverse relaxation model.[21] It was shown that for vesicle radii $R_0 \geq 200$ nm translational diffusion of the lipid molecules along the vesicle shell is too slow to contribute significantly to transverse spin relaxation in the kHz range, whereas vesicle shape fluctuations constitute the dominant transverse relaxation process.[21]

Hydrodynamic Model. The model of shape fluctuations of quasi-spherical vesicles was developed by Milner and Safran[26] on the basis of Helfrich's theory of the elasticity of lipid bilayers[27] and the hydrodynamic approach of Schneider et al.[2] In this model, a vesicle is considered to be a quasi-spherical closed shell of radius R_0 characterized by a fixed volume $V = 4\pi R_0^3/3$ and a fixed area A. The vesicle is assumed to be flaccid, a fact that may be described by the dimensionless excess area Δ:[28]

$$A = (4\pi + \Delta)R_0^2 \tag{3}$$

Apart from the bending rigidity of the membrane, the excess area is an important parameter characterizing the shape and the thermal fluctuations of a vesicle.

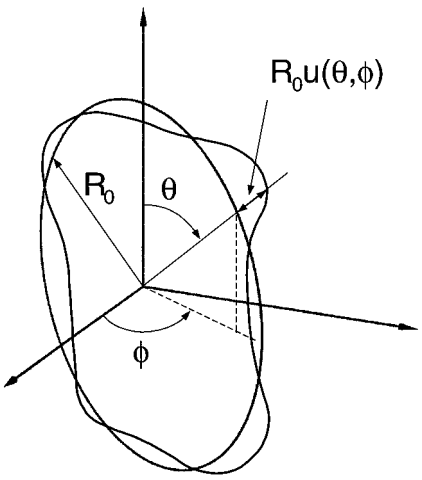

Figure 6. Schematic representation of shape fluctuations of quasi-spherical vesicles. θ and ϕ denote the polar and azimuthal angles, respectively, of the considered surface point with respect to an arbitrary reference system. $R_0u(\theta, \phi)$ characterizes the radial deviation from the spherical conformation.

For quantitative modeling of the fluctuations, the vesicle is described by a slightly deformed spherical surface as (see Figure 6)

$$R(\theta, \phi) = R_0(1 + u(\theta, \phi)) \tag{4}$$

where $u(\theta, \phi)$ is a dimensionless parameter characterizing the radial deviation from the spherical conformation. θ and ϕ denote the polar and azimuthal angles, respectively, of the considered surface point with respect to an arbitrary reference system (see Figure 6). The displacement of the membrane $u(\theta, \phi)$ generates a curvature and consequently a deflection of the local membrane normal away from its average orientation in the radial direction (see Figure 6). The unit vector $\vec{n} \simeq (n_\theta, n_\phi, 1)$ representing the instantaneous direction of the local membrane normal corresponds to the well-known director in thermotropic liquid crystals.

Using a small-angle approximation, the time autocorrelation function for n_θ and n_ϕ can be written as[20, 21]

$$\overline{n_\theta(0)n_\theta(t)} = \overline{n_\phi(0)n_\phi(t)} = \sum_{l=2}^{l_{max}} \sigma_l^2 \exp(-t/\tau_l) \tag{5}$$

$$\sigma_l^2 = \frac{1}{8\pi} l(l+1)(2l+1)\overline{u_{l,m}^2} \tag{6}$$

where the mean-square amplitude and relaxation time for each mode are given by[2,26]

$$\overline{u_{l,m}^2} = \frac{k_B T}{\kappa} \frac{1}{(l+2)(l-1)(l^2+l+\sigma)} \tag{7}$$

$$\tau_l = \frac{\eta R_0^3}{\kappa} \frac{(2l+1)(2l^2+2l-1)}{(l-1)l(l+1)(l+2)(l^2+l+\sigma)} \tag{8}$$

Here, η is the viscosity of the surrounding fluid, κ is the bending elastic modulus of the membrane, and σ is the dimensionless effective lateral tension that is related to the excess area Δ by the implicit equation[8,28]

$$\Delta = \frac{k_B T}{2\kappa} \sum_{l=2}^{l_{max}} \frac{2l+1}{l^2+l+\sigma} \tag{9}$$

According to Milner and Safran, the summation over l in eqs 5 and 9 is extended from $l = 2$ to $l_{max} \simeq \pi R_0/a$ where a is the average intermolecular distance.[26] The expressions for the time autocorrelation functions of n_θ and n_ϕ (i.e., eqs 5−8) are the basis for an analytical expression of the transverse rate, $R_2^{CP}(\omega)$, in a CP multipulse sequence.[21]

Transverse Relaxation Model. Vesicle shape fluctuations are characterized by a broad distribution of thermally activated modes extending over a wide frequency range down to the kHz regime.[20,21,26] Consequently, a rigorous analysis of the transverse relaxation induced by these fluctuations is generally hampered by the lack of time scale separation between the slow elastic modes and the transverse magnetization decay. Under these conditions, the use of a fast-motion theory[20] is no longer justified, and one should resort to a slow-motional approach based on the stochastic Liouville equation.[29] Such a formal treatment of the dynamic problem has been presented in the preceding paper for the specific case of ^{31}P nuclei in the headgroups of lipid molecules forming unilamellar vesicles.[21]

An analytical solution of the stochastic Liouville equation is obtained if the vesicle fluctuations are modeled as a multidimensional Gaussian process. As a matter of fact, such a representation can be adopted for the fluctuating local membrane normal (see Figure 6) using a small-angle approximation that is consistent with the linear approximation employed for the modulated spin Hamiltonian.[21,29] In this way, one can derive an analytical expression for the relaxation rate, $R_{2,n}^{CP}(\omega)$, on the basis of the relative decrease of the transverse magnetization during cycle n:[29]

$$R_{2,n}^{CP}(\omega) = -\frac{1}{2\tau} \ln \frac{M(2n\tau)}{M(2(n-1)\tau)} \tag{10}$$

Generally, the dependence of $R_{2,n}^{CP}(\omega)$ on the number of cycles n in the CP sequence is rather weak.[29] Consequently, one can interpret the experimental data in terms of an asymptotic relaxation rate referring to an infinite sequence, $R_{2,\infty}^{CP}(\omega) = \lim_{n\to\infty} R_{2,n}^{CP}(\omega)$. For such a relaxation rate, the following compact result has been obtained:[21]

$$R_{2,\infty}^{CP}(\omega) = \frac{1}{T_2^0} + 16\pi^2 \left(\frac{\Delta\nu_{obs}}{S_{ODF}}\right)^2 \sin^2\theta_B \cos^2\theta_B \sum_{l=2}^{l_{max}} \sigma_l^2 \times \tau_l[1 - (\tau_l\omega)\tanh(\tau_l\omega)^{-1}] \tag{11}$$

$(T_2^0)^{-1}$ is the contribution from the fast molecular motions, $\Delta\nu_{obs}$ is the observed splitting defined as the full width of the experimental ^{31}P NMR spectrum (see Figure 2), and S_{ODF} is the order parameter of the fluctuating local membrane normal written as

$$S_{ODF} = 1 - 3\sum_{l=2}^{l_{max}} \sigma_l^2 \tag{12}$$

Notably, the analytical expression for the transverse relaxation rate is the same as that employed previously on the basis of a fast-motion theory.[11,12]

In deriving eq 11, only linear contributions of the orthogonal components of the fluctuating membrane normal have been employed. Consequently, the theory cannot account for orienta-

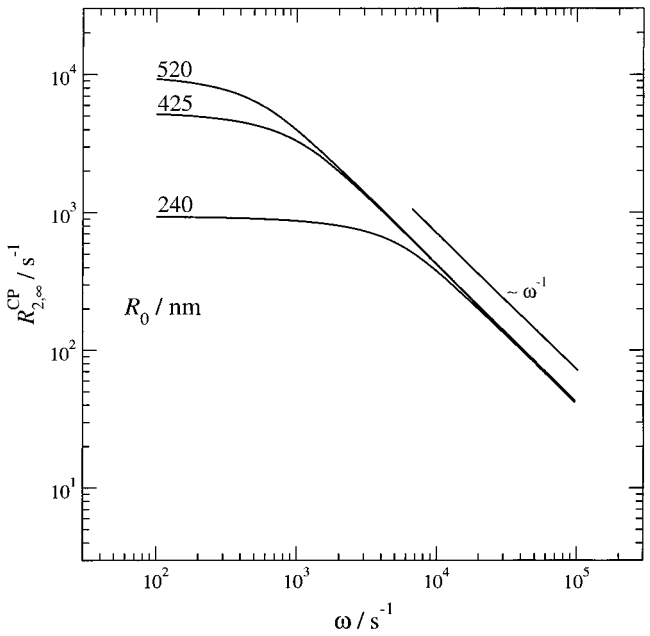

Figure 7. Dependence of the calculated transverse ^{31}P nuclear spin relaxation rate $R^{CP}_{2,\infty}(\omega)$ on the pulse frequency ω in a Carr−Purcell sequence for shape fluctuations of quasi-spherical vesicles. The dispersion profiles refer to $R_0 = 240$ nm, 425 nm, and 520 nm and a splitting of $\Delta\nu_{obs} = 5$ kHz. The other parameters used in the plot are bending elastic modulus $\kappa = 4 \times 10^{-20}$ J; lateral tension $\sigma = 0$; viscosity $\eta = 6.5 \times 10^{-4}$ Pa s; and intermolecular distance $a = 1$ nm.

tions in which the average director is either parallel or perpendicular to the magnetic field (i.e., $\theta_B = 0°, 90°$). In such cases, consideration of the bilinear terms of the director field would be required.[29]

In Figure 7, the pulse frequency dependence of $R^{CP}_{2,\infty}(\omega)$ given in eq 11 is depicted for the three different vesicle sizes studied in this work. The dispersion profiles refer to the $\theta_B = 45°$ orientation and a vanishing molecular contribution of $1/T_2^0 = 0.0$. One sees that $R^{CP}_{2,\infty}(\omega)$ depends linearly on ω^{-1} over a wide frequency range in the kHz regime. Notably, within this linear dispersion regime, the magnitude of $R^{CP}_{2,\infty}(\omega)$ is independent of the size of the vesicle R_0. As shown earlier,[20,21] it is also independent of the effective lateral tension σ and the viscosity of the surrounding fluid η, leaving the bending elastic modulus κ as the only relevant parameter. On the other hand, R_0, σ, η, and κ determine the frequency at which $R^{CP}_{2,\infty}(\omega)$ levels off to a constant plateau value that is independent of ω. As the values of R_0 and η are determined by other methods, a careful analysis of the experimental dispersion profiles (see Figures 4 and 5) can provide reliable values for κ and σ.

Evaluation of Viscoelastic Properties. Values for the viscoelastic parameters κ and σ were obtained from the computational analysis of the experimental dispersion profiles (see Figures 4 and 5). The underlying fixed parameters are summarized in Table 1 (rows 1−6). Values for $\Delta\nu_{obs}$ were extracted from the experimental ^{31}P NMR spectra (see Figure 2). The value for η corresponds to the viscosity of water and is consistent with the value from the applied hydrodynamic model.[2,26] Values for the vesicle radius R_0 were determined by dynamic light scattering (see section 2). For the average intermolecular distance, a value of $a = 1$ nm has been assumed (see eqs 5, 9, 11, and 12).

Calculated dispersion profiles (see eq 11) were fitted to the experimental profiles by varying the parameters κ and σ. In the calculations, contributions from the fast molecular motions ($1/T_2^0 = 0.0$) have been neglected. The solid lines in Figures 4 and 5 represent the best simulations of the dispersion profiles on the basis of the parameter values listed in Table 1 (rows 7 and 8). Evidently, the agreement is very good. The uniqueness of the fit was tested by running the fit procedure with different starting values. Within the error limits, the same values for κ and σ were obtained. The cited errors are linear confidence limits that refer to a confidence level of 0.95.

The evaluated values for κ vary by 1 order of magnitude over the range of $(1.5 \pm 0.1) \times 10^{-20}$ J to $(8.3 \pm 0.1) \times 10^{-20}$ J and thus correspond to previous results obtained by video microscopy,[2−8] micropipetting,[30] and electric deformation techniques.[31,32] Inspection of Table 1 reveals that the value of κ sensitively depends on the temperature of the sample. Evidently, κ increases by a factor of 2 when the temperature is lowered by 10 K.[33] In addition, there is a significant increase of the bending elastic modulus if H_2O is used instead of HEPES buffer. These findings indicate that a comparison of measured κ values is meaningful only if they refer to the same experimental conditions.

From the plateau in the dispersion profiles of the pure DMPC vesicles, values for the effective lateral tension of $\sigma = 3 \pm 1$ and $\sigma = 4 \pm 1$ have been extracted. These values are somewhat smaller than those reported in the literature.[28] Because a plateau is not observed in the dispersion profiles of the DMPC/cholesterol vesicles, only rough estimates for σ could be evaluated (Table 1, row 8).

The parameters κ and σ have been used to evaluate the excess area $\Delta A/A_{sphere} = \Delta/4\pi$ (see eq 9), which is an important quantity characterizing the shape and the thermal fluctuations of a vesicle.[8,28] In fact, $\Delta A/A_{sphere}$ specifies the deviation of the shape of the vesicle from a sphere of the same volume. One sees that the excess area of the studied vesicles varies between $\Delta A/A_{sphere} = 0.03$ and 0.13, indicating a strong modulation of the rigidity of the vesicles by the bilayer composition and the temperature (Table 1, row 9).

This bending rigidity can also be expressed in terms of the order parameter S_{ODF} of the fluctuating membrane normal. Values for S_{ODF} have been evaluated from the viscoelastic parameters κ and σ according to eq 12. One sees that S_{ODF} varies between $S_{ODF} = 0.60$ and 0.92 depending on the bilayer composition and the temperature (Table 1, row 10).

5. Discussion

Relaxation Mechanism. In the previous section, we evaluated viscoelastic parameters of membrane vesicles while assuming that vesicle shape fluctuations constitute the dominant transverse relaxation process. It is appropriate at this point to examine in more detail the grounds for adopting this relaxation mechanism. In principle, one might expect that translationally induced rotations[34] of lipid molecules also contribute to the transverse relaxation process. The corresponding rotational correlation time, τ_{rot}, is related to the translational diffusion coefficient, D^{transl}, of the lipid molecule by[34]

$$\tau_{rot} = \frac{R_0^2}{6D^{transl}} \tag{13}$$

where R_0 denotes the average radius of the vesicle. A value of $D^{transl} = 5 \times 10^{-12}$ m^2 s^{-1} is generally accepted in the literature.[35]

The vesicle radii of the pure DMPC samples (i.e., $R_0 = 240$ and 425 nm) display effective rotational correlation times of approximately 2−6 ms. These values place the lateral diffusion process in the slow-motional regime. An appropriate relaxation

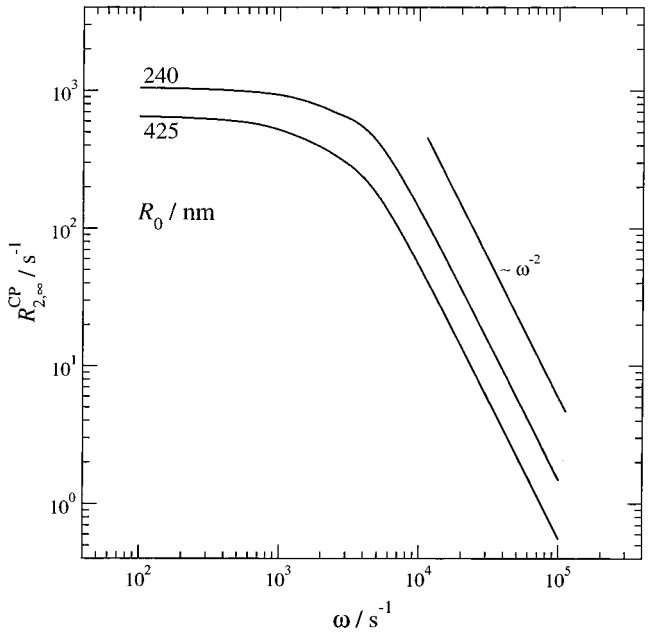

Figure 8. Dependence of the calculated transverse ^{31}P nuclear spin relaxation rate $R^{CP}_{2,\infty}(\omega)$ on the pulse frequency ω in a Carr−Purcell sequence for translational lipid diffusion. The dispersion profiles refer to $R_0 = 240$ nm and 425 nm and a residual magnetic anisotropy of 5.34 kHz. The assumed translational diffusion coefficient is $D^{transl} = 5 \times 10^{-12}$ m^2 s^{-1}.

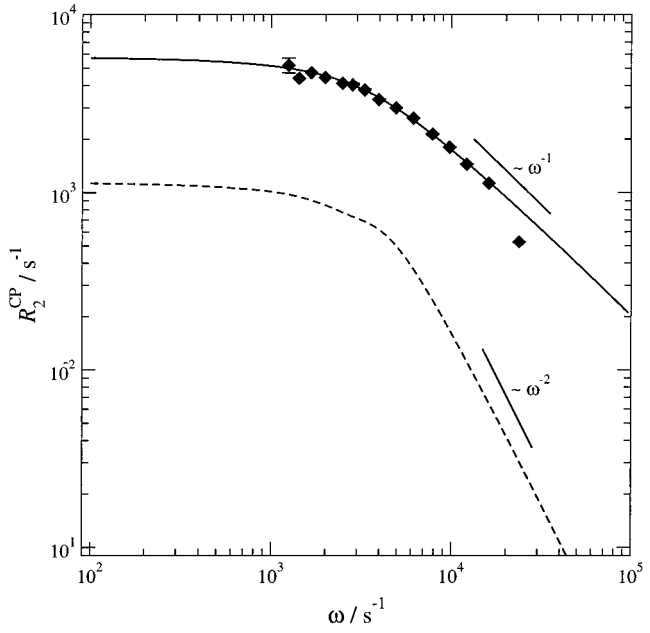

Figure 9. Dependence of the transverse ^{31}P nuclear spin relaxation rate $R^{CP}_{2}(\omega)$ on the pulse frequency ω in a Carr−Purcell sequence for two different relaxation mechanisms: vesicle shape fluctuations (experimental data points, —) and translationally induced rotations (− − −)). The dispersion profiles refer to the same vesicle radius of $R_0 = 240$ nm. The assumed translational diffusion constant is $D^{transl} = 5 \times 10^{-12}$ m^2 s^{-1}. All other parameters used in the plot are listed in Table 1.

model has been described in the preceding paper.[21] Figure 8 shows calculated $R^{CP}_{2,\infty}(\omega)$ dispersion profiles for the two different radii, assuming that translationally induced rotations represent the unique transverse relaxation process. The employed residual magnetic anisotropy of 5.34 kHz has been extracted from the experimental powder spectra (see Figure 2).[21]

Clearly, both relaxation curves exhibit a characteristic dispersion with a plateau at low frequencies and an inverse square dependence of $R^{CP}_{2,\infty}(\omega) \propto \omega^{-2}$ at higher frequencies. The fact that this behavior is *not* observed experimentally indicates that, at least for vesicles with $R_0 \geq 200$ nm, lateral diffusion does not represent the major spin relaxation mechanism (see Figure 4). Additionally, experimental nuclear spin relaxation rates, $R^{CP}_{2}(\omega)$, for vesicles with distinct radii are found to be virtually indistinguishable over a wide range of pulse frequencies (see Figure 4). In view of the notable difference in size (a factor of 1.6) and the corresponding difference in the respective rotational correlation times (a factor of 3), this result is further evidence for some other mechanism dominating transverse spin relaxation. From the observed linear dependence ($R^{CP}_{2}(\omega) \propto \omega^{-1}$), one can conclude that thermally excited vesicle shape fluctuations constitute the major transverse relaxation process (see Figure 4).

Evidently, translational lipid diffusion is too slow to contribute significantly to transverse relaxation in the kHz range. This is demonstrated in Figure 9, where we compare an experimental R^{CP}_{2} dispersion profile (filled diamonds, solid line) with that calculated for lateral lipid diffusion (dashed line). The relaxation curves refer to a vesicle radius of $R_0 = 240$ nm. One sees that lateral diffusion across the vesicle shell makes only a minor contribution to the transverse relaxation rates, in contrast to previous suggestions.[36,37] The same is true for contributions from the tumbling motion of the vesicle as a whole.

Interbilayer Coupling. It is appropriate to make a few comments here concerning the strength of interbilayer coupling in oligo- and multilamellar membranes. To our knowledge, reliable experimental data for these interactions do not exist. Figure 4 shows that the relaxation rates $R^{CP}_{2}(\omega)$ are, within the linear dispersion regime, the same for the unilamellar and the oligolamellar vesicles, which indicates that the individual bilayers in an oligolamellar vesicle fluctuate incoherently down to a frequency of about 10 kHz. Apparently, the coupling between the bilayers in these vesicles is extremely weak.

A linear dispersion of $R^{CP}_{2}(\omega)$ in the lower kHz regime was also observed for multilamellar stacks of planar membranes.[14,38,39] It was pointed out earlier that in this case spin relaxation is due to undulations of a free planar membrane.[16] In reality, however, it is difficult to estimate the conditions under which free-membrane undulations occur in a multilamellar stack because this estimation requires knowledge of the transverse orientational correlation length, λ_p, given by

$$\lambda_p = \left(\frac{\kappa d'}{B}\right)^{1/4} \tag{14}$$

where d' is the bilayer repeat distance and B is the compression modulus. According to a previous conjecture, B might be large enough to restrict the linear dispersion of $R^{CP}_{2}(\omega)$ to the MHz regime.[18] Even though the range of the linear dispersion depends to some extent on the dispersion relation for the damping times of the fluctuation modes, our data certainly imply much smaller values for the compression modulus than previously anticipated.[18]

Dynamics of Vesicle Fluctuations. Analysis of the low-frequency cutoff of the experimental R^{CP}_{2} dispersion profiles provides valuable information about the dynamics of the vesicle fluctuations. Because strong dissipation arises from the viscous damping in the surrounding fluid, these fluctuations are overdamped.[42] On the basis of previous work,[2] Milner and Safran derived a dispersion relation for the damping times τ_l of the elastic modes that is given in eq 8.[26] Using this dispersion relation, excellent agreement has been obtained between ex-

TABLE 2: Bending Elastic Moduli of DMPC Membrane Vesicles Obtained by Different Methods

system	sample	temperature T/K	bending elastic modulus $\kappa/10^{-20}$ J	method	reference
DMPC/HEPES[a] buffer	oligolamellar vesicles	313	1.5	transverse NMR relaxation	this work
DMPC/HEPES[a] buffer	oligolamellar vesicles	303	2.7	transverse NMR relaxation	this work
DMPC/H_2O	oligolamellar vesicles	303	4.6	transverse NMR relaxation	this work
DMPC/H_2O	oligolamellar dispersion	303	5.4[b]	transverse NMR relaxation	12
DMPC/H_2O	giant vesicles	302	5.6	micropipet	30
DMPC/H_2O	giant vesicles	299	3.5−6.5	video microscopy	3
DMPC/H_2O	giant vesicles	303	11.5	video microscopy	6
DMPC/H_2O	giant vesicles	303	13.0	video microscopy	7

[a] HEPES: 2-[4-(2-hydroxyethyl)-1-piperazino]ethanesulfonic acid. [b] Corrected value corresponding to $^2/_3$ of the published value on the basis of the assumption of quasi-planar membrane fluctuations. The factor $^2/_3$ arises from the employed dispersion relation for the damping times of the elastic modes.[21]

TABLE 3: Bending Elastic Moduli of Various Lipid Vesicles Obtained by Pulse Frequency-Dependent Transverse ^{31}P NMR Relaxation

system	sample	temperature T/K	bending elastic modulus[b] $\kappa/10^{-20}$ J	reference
DMPC/H_2O	oligolamellar dispersion	313	3.8	12
DMPC/15% cholesterol/H_2O	oligolamellar dispersion	313	11.2	12
DMPC/40% cholesterol/H_2O	oligolamellar dispersion	313	24.0	11,12
DMPC/HEPES[a] buffer	oligolamellar dispersion	313	2.6	11
DMPC/4% gramicidin/HEPES[a] buffer	oligolamellar dispersion	313	4.4	11,12
DMPC/1.12% rhodopsin/HEPES[a] buffer	oligolamellar dispersion	313	2.4	12

[a] HEPES: 2-[4-(2-hydroxyethyl)-1-piperazino]ethanesulfonic acid. [b] Corrected values corresponding to $^2/_3$ of the published values on the basis of the assumption of quasi-planar membrane fluctuations. The factor $^2/_3$ arises from the employed dispersion relation for the damping times of the elastic modes.[21]

perimental and calculated R_2^{CP} relaxation curves (see Figure 4). On the basis of this result, we can conclude that the dynamics of the vesicle fluctuations investigated by the CP experiments is adequately described by the relation (eq 8).

In the derivation of eq 8, however, the bilayer architecture has been ignored. The analysis of the fluctuations of a planar membrane has shown that the coupling between the shape and density difference modifies the damping times for wavevectors $q_\perp$ that are larger than a crossover wavevector $q_{\perp 1}$.[43] Rough estimates indicate that $q_{\perp 1}$ corresponds to a wavelength in the micrometer range. For shorter wavelengths, bending modes are so fast that the lipid density can no longer accommodate the shape because intermonolayer friction provides an additional dissipative mechanism.[43] Because of the coupling between shape and lipid density, the correlation function for a single mode no longer decays as a simple exponential but rather involves two damping times in this regime.[43] Taking into account the same phenomenon in spherical geometry, one can expect significant deviations from eq 8. It should be noted that transverse NMR relaxation studies involving CP sequences represent a powerful tool for the assessment of the dispersion relation because it significantly affects the low-frequency cutoff of the relaxation curve.[20]

Bending Rigidity. There are several methods for determining the bending rigidity κ of vesicles. In the "flickering" experiments, the bending rigidity is determined from mean-square amplitudes of thermally excited vesicle shape fluctuations using phase contrast microscopy with fast image processing.[2−8] In the micropipet technique, the strength of the fluctuations is mechanically controlled. From the relation between the area stored in the fluctuations and the suction pressure, the bending rigidity can be deduced.[30]

The κ values obtained by these techniques are compared in Table 2 with those evaluated by transverse NMR relaxation using CP sequences. All bending moduli refer to pure DMPC vesicles that are dispersed either in HEPES buffer or in water. Provided the same experimental conditions are used, the κ values from NMR compare favorably with those obtained by other techniques. In some cases, however, the bending rigidity differs by a factor of 2. Whether these discrepancies are attributable to experimental problems or real physical effects needs further analysis. Notably, the NMR measurements are performed on quasi-spherical vesicles whose radii are nearly 2 orders of magnitude smaller than those employed in video microscopy. This difference might be relevant in view of the conjectured dependence of the bending elastic modulus on the wavelength of the elastic deformations.[44]

Evidently, transverse NMR relaxation is well-suited to the study of the bending rigidity of vesicles. First, the values for κ can be extracted from the linear regime of the dispersion profile, where the relaxation rate is independent of the radius of the vesicle R_0 and the effective lateral tension σ (see Figure 7). Second, there is no need to prepare giant unilamellar vesicles such as in video microscopy.[2−8] Rather, oligolamellar lipid dispersions with a broad distribution of vesicle radii[45] can be studied by the NMR technique.[10−12]

Table 3 summarizes the results of previous ^{31}P NMR studies performed on oligolamellar lipid dispersions with varying bilayer compositions.[11,12] From the values of κ it can be seen that cholesterol causes a stiffening of the membrane vesicles, increasing the bending elastic modulus substantially.[6] Low concentrations of gramicidin have a similar but less pronounced effect, whereas rhodopsin, an integral membrane protein, fluidizes the vesicle. The change in κ for this system, however, is very small.

The values obtained for κ are reasonable and indicate that transverse nuclear spin relaxation is able to provide information concerning viscoelastic properties in biological membranes. Of particular importance from a biological point of view is that the technique may be exploited to investigate modifications of membrane viscoelastic behavior caused by included sterols, peptides, or proteins. Indeed, the results presented in Table 3 suggest that these effects are by no means small and invite speculation regarding the consequences for overall membrane function.

6. Conclusions

Pulse frequency-dependent measurements of the transverse CP nuclear spin relaxation rates, $R_2^{CP}(\omega)$, provide detailed information on the slow-motional dynamics in membrane vesicles with controlled radii, R_0. The observed relaxation rates exhibit a linear dependence on ω^{-1} over a wide frequency range in the kHz regime and then level off to a constant plateau value independent of ω. Within the linear dispersion regime, the same relaxation rates are detected for unilamellar and oligolamellar vesicles, which indicates that the interbilayer coupling is weak and has no effect on the measured relaxation curves.

Analysis of the experimental dispersion profiles is performed using a comprehensive NMR relaxation model[29] developed for ^{31}P nuclei in the headgroups of lipid molecules forming quasi-spherical vesicles.[21] The basis of the model is the stochastic Liouville equation in which two different relaxation processes are considered: vesicle shape fluctuations[26] and molecular translational diffusion.[34] We have shown that for vesicle radii $R_0 \geq 200$ nm lateral diffusion across the vesicle shell is too slow to contribute significantly to transverse spin relaxation in the kHz range, whereas vesicle shape fluctuations constitute the dominant transverse relaxation process.

Model calculations reveal that $R_2^{CP}(\omega)$, induced by vesicle fluctuations, depends linearly on ω^{-1} over a wide frequency range in the kHz regime. Notably, within this linear dispersion regime, the bending elastic modulus κ is the only relevant parameter because the magnitude of $R_2^{CP}(\omega)$ does not depend on the size of the vesicle R_0, the effective lateral tension σ, or the viscosity of the surrounding fluid η. On the other hand, R_0, σ, η, and κ determine the frequency at which $R_2^{CP}(\omega)$ levels off to a constant plateau value that is independent of ω.

Thus, analysis of the linear dispersion regime provides a direct way to determine the bending elastic modulus κ of the membranes. For the studied DMPC and DMPC/cholesterol vesicles dispersed in excess aqueous buffer, the κ values vary by 1 order of magnitude over the range of $(1.5 \pm 0.1) \times 10^{-20}$ J to $(8.3 \pm 0.1) \times 10^{-20}$ J and thus correspond to results obtained by other techniques.[3,6,7,30] In addition, the new approach can be used to determine the effective lateral tension σ in the vesicles. From the plateau in the experimental dispersion profiles, values of $\sigma = 3 \pm 1$ and $\sigma = 4 \pm 1$ are extracted.

Evidently, transverse CP nuclear spin relaxation represents a powerful tool for the evaluation of the bending rigidity of vesicles. First, the value of κ can easily be extracted from the linear regime of the $R_2^{CP}(\omega)$ dispersion profile where κ is the only adjustable parameter. Second, there is no need to prepare giant unilamellar vesicles such as in video microscopy.[2−8] Rather, oligolamellar lipid dispersions with a broad distribution of vesicle radii can be studied by the NMR technique.[10−12] This technique is particularly useful for studies of the modulation of the bending rigidity by different membrane constituents such as cholesterol, peptides, or proteins.[11,12]

Acknowledgment. Financial support by the Deutsche Forschungsgemeinschaft (SFB 428; D2 and D4) is gratefully acknowledged. M.V. acknowledges the support by the Ministry of Science and Technology of Slovenia. We thank the EU Commission for their support through the TMR Program Contract FMRX CT97 0121.

References and Notes

(1) *Structure and Dynamics of Membranes*; Lipowsky, R., Sackmann, E., Eds.; Elsevier: Amsterdam, The Netherlands, 1995.
(2) Schneider, M. B.; Jenkins, J. T.; Webb, W. W. *J. Phys. (Paris)* **1984**, *45*, 1457.
(3) Engelhardt, H.; Duwe, H. P.; Sackmann, E. *J. Phys. Lett.* **1985**, *46*, 395.
(4) Bivas, I.; Hanusse, P.; Bothorel, P.; Lalaune, J.; Aquerre-Chariol, O. *J. Phys. (Paris)* **1987**, *48*, 855.
(5) Faucon, J. F.; Mitov, M. D.; Méléard, P.; Bivas, I.; Bothorel, P. *J. Phys. (Paris)* **1989**, *50*, 2389.
(6) Duwe, H. P.; Kaes, J.; Sackmann, E. *J. Phys. (Paris)* **1990**, *51*, 945.
(7) Méléard, P.; Gerbeaud, C.; Pott, T.; Fernandez-Puente, L.; Bivas, I.; Mitov, M. D.; Dufourc, J.; Bothorel, P. *Biophys. J.* **1997**, *72*, 2616.
(8) Häckl, W.; Seifert, U.; Sackmann, E. *J. Phys. II* **1997**, *7*, 1141.
(9) Rommel, E.; Noack, F.; Meier, P.; Kothe, G. *J. Phys. Chem*. **1988**, *92*, 2981.
(10) Dufourc, E.; Mayer, C.; Stohrer, J.; Althoff, G.; Kothe, G. *Biophys. J.* **1992**, *61*, 42.
(11) Kothe, G.; Heaton, N. J. In *Encyclopedia of Nuclear Magnetic Resonance*; Grant, D. M., Harris, R. K., Eds.; John Wiley: Chichester, U.K., 1996; Vol. 7, pp 4436−4444.
(12) Althoff, G.; Heaton, N. J.; Gröbner, G.; Prosser, R. S.; Kothe G. *Colloids Surf., A* **1996**, *115*, 31.
(13) Noack, F. *Prog. Nucl. Magn. Reson. Spectrosc*. **1986**, *18*, 171.
(14) Stohrer, J.; Gröbner, G.; Reimer, D.; Weisz, K.; Mayer, C.; Kothe, G. *J. Chem. Phys*. **1991**, *95*, 672.
(15) Carr, H. Y.; Purcell, E. M. *Phys. Rev.* **1954**, *94*, 630. Meiboom, S.; Gill, D. *Rev. Sci. Instrum.* **1958**, *29*, 688.
(16) Marqusee, J. A.; Warner, M.; Dill, K. A. *J. Phys. Chem.* **1984**, *81*, 6404.
(17) Blinc, R.; Luzar, M.; Vilfan, M.; Burgar, M. *J. Chem. Phys.* **1975**, *63*, 3445.
(18) Halle, B. *Phys. Rev. E* **1994**, *50*, R2415.
(19) Halle, B.; Gustafsson, S. *Phys. Rev. E* **1997**, *56*, 690.
(20) Vilfan, M.; Althoff, G.; Vilfan, I.; Kothe, G. *Phys. Rev. E* **2001**, *64*, 022902.
(21) Althoff, G.; Frezzato, D.; Vilfan, M.; Stauch, O.; Schubert, R.; Vilfan, I.; Moro, G. J.; Kothe, G. *J. Phys. Chem. B* **2002**, *106*, 5506.
(22) Bartlett, G. R. *J. Biol. Chem*. **1959**, *234*, 460.
(23) Dufourc, E. J.; Mayer, C.; Stohrer, J.; Kothe, G. *J. Chim. Phys.* **1992**, *89*, 243.
(24) Press, W. H.; Teukolsky, S. A.; Vetterling, W. T.; Flannery, B. P. *Numerical Recipes in Fortran: The Art of Scientific Computing*, 2nd ed.; Cambridge University Press: Cambridge, U.K., 1992.
(25) Brandt, S. *Datenanalyse*, 3rd ed.; Bibliographisches Institut: Mannheim, Germany, 1992.
(26) Milner, S. T.; Safran, S. A. *Phys. Rev. A* **1987**, *36*, 4371.
(27) Helfrich, W. *Z. Naturforsch*. **1973**, *28*, 693.
(28) Seifert, U.; Lipowsky, R. In *Structure and Dynamics of Membranes*; Lipowsky, R., Sackmann E., Eds.; Elsevier: Amsterdam, The Netherlands, 1995; pp 403−464.
(29) Frezzato, D.; Kothe, G., Moro, G. *J. Phys. Chem. B* **2001**, *105*, 1281.
(30) Evans, E.; Rawiecz, W. *Phys. Rev. Lett*. **1990**, *64*, 2094.
(31) Kummrow, M.; Helfrich, W. *Phys. Rev. A* **1991**, *44*, 8356.
(32) Niggemann, G.; Kummrow, M.; Helfrich, W. *J. Phys. II* **1995**, *5*, 413.
(33) A similar temperature effect has been observed previously (ref 32).
(34) Zumer, S.; Vilfan, M. *J. Phys*. **1985**, *46*, 1763. Halle, B. *J. Chem. Phys.* **1991**, *94*, 3150.
(35) Lindblom, G.; Johansson, L. B.-A.; Arvidson, G. *Biochemistry* **1981**, *20*, 2204.
(36) Bloom, M.; Sternin, E. *Biochemistry* **1987**, *26*, 2101.
(37) Dolainsky, C.; Möps, A.; Bayerl, T. M. *J. Chem. Phys*. **1993**, *98*, 1712.
(38) Liesum, L. Diploma Thesis, University of Freiburg, 1996.
(39) It should be noted that multilamellar stacks of planar membranes are notoriously difficult to hydrate.[40,41]
(40) Rand, R. P.; Parsegian, V. A. *Biochim. Biophys. Acta* **1989**, *988*, 351.
(41) Podgornik, R.; Parsegian, V. A. *Biophys. J.* **1997**, *72*, 942.
(42) Brochard, F.; Lennon, J. F. *J. Phys. (Paris)* **1975**, *36*, 1035.
(43) Seifert, U.; Langer, S. A. *Europhys. Lett.* **1993**, *23*, 71.
(44) Helfrich, W. In *Structure and Dynamics of Membranes*; Lipowsky, R., Sackmann, E., Eds.; Elsevier: Amsterdam, The Netherlands, 1995; pp 691−721.
(45) Heaton, N. J.; Althoff, G.; Kothe, G. *J. Phys. Chem.* **1996**, *100*, 4944.